Proteome aggregation in cells derived from amyotrophic lateral sclerosis patients for personalized drug evaluation

Carmen Pérez de la Lastra Aranda, Carlota Tosat-Bitrián, Gracia Porras, Ruxandra Dafinca, Diego Muñoz-Torrero, Kevin Talbot, Ángeles Martín-Requero, Ana Martínez, and Valle Palomo*

Proteome aggregation in cells derived from amyotrophic lateral sclerosis patients for personalized drug evaluation

Carmen Pérez de la Lastra Aranda[1], Carlota Tosat-Bitrián[2], Gracia Porras[2], Ruxandra Dafinca[3,4] Diego Muñoz-Torrero[5], Kevin Talbot[3,4], Ángeles Martín-Requero[2,6], Ana Martínez[2,6], Valle Palomo*[,1,6,7].

[1] Instituto Madrileño de Estudios Avanzados en Nanociencia (IMDEA Nanociencia), C/ Faraday 9, 28049, Madrid, Spain

[2] Centro de Investigaciones Biológicas "Margarita Salas"-CSIC, Ramiro de Maeztu 9, 28040 Madrid, Spain

[3] Oxford Motor Neuron Disease Centre, Nuffield Department of Clinical Neurosciences, University of Oxford, John Radcliffe Hospital, Oxford, OX3 9DU UK.

[4] Kavli Institute for Nanoscience Discovery, University of Oxford, Dorothy Crowfoot Hodgkin Building, Oxford, OX1 3QU UK.

[5] Laboratory of Medicinal Chemistry (CSIC Associated Unit), Faculty of Pharmacy and Food Sciences, and Institute of Biomedicine (IBUB), University of Barcelona (UB), Av. Joan XXIII 27-31, E-08028 Barcelona, Spain.

[6] Centro de Investigación Biomédica en Red en Enfermedades Neurodegenerativas, (CIBERNED), Instituto de Salud Carlos III, Av. Monforte de Lemos, 3-5, 28029 Madrid, Spain.

[7] Unidad Asociada al Centro Nacional de Biotecnología (CSIC), Darwin 3, 28049 Madrid, Spain

Corresponding author email: valle.palomo@imdea.org

ABSTRACT

Amyotrophic lateral sclerosis (ALS) is a progressive neurodegenerative disorder that currently lacks effective therapy. Given the heterogeneity of clinical and molecular profiles of ALS patients, personalized diagnostics and pathological characterization represent a powerful strategy to optimize patient stratification, thereby enabling a personalized treatment. Immortalized lymphocytes from sporadic and genetic ALS

patients recapitulate some pathological hallmarks of the disease, facilitating the fundamental task of drug screening. However, the molecular aggregation of ALS has not been characterized in this patient-derived cellular model. Indeed, protein aggregation is one of the most prominent features of neurodegenerative diseases, and therefore models to test drugs against personalized pathological aggregation could help discover improved therapies. With this work, we aimed to characterize the aggregation profile of ALS immortalized lymphocytes and test several drug candidates with different mechanisms of action. In addition, we have evaluated the molecular aggregation in motor neurons derived from two hiPSC cell lines corresponding to ALS patients with different mutations in *TARDBP*. The results provide a valuable insight on the different characterization of sporadic and genetic ALS patients' immortalized lymphocytes, their differential response to drug treatment, and the usefulness of proteome homeostasis characterization in patients' cells.

KEYWORDS

Amyotrophic lateral sclerosis, protein aggregation, turbidity, patient samples, personalized drug evaluation

INTRODUCTION

Amyotrophic lateral sclerosis (ALS) is a syndrome with a spectrum of clinical phenotypes characterized by progressive paralysis and ultimately death, typically from respiratory failure. The biological determinants of ALS are complex, but key molecular pathological features include protein aggregation, excitotoxicity, inflammation and oxidative stress, that ultimately result in progressive degeneration of upper and lower motor neurons. [1] The biological basis of clinical heterogeneity in ALS is poorly understood, which is one of a number of factors impeding the discovery of effective therapeutic agents. [2]

Molecular phenotyping of ALS is likely to aid personalized diagnosis and facilitate clinical trials by providing a rational framework for sub-stratification. Pre-clinical models based

on cells derived from patients represent a potentially powerful platform for improving our understanding of biological heterogeneity and for testing therapeutic strategies [3], [4]. Motor neurons derived from induced pluripotent stem cells (iPSC) recapitulate some molecular pathological features of the disease, though phenotypes can be subtle, and differentiation is time-consuming and expensive, limiting their value for high-throughput screening. [5],[6]. Direct reprogramming from fibroblasts has the potential to yield neurons that may conserve some of the pathological characteristics of ALS, but the long duration of this methodology similarly impedes its practical use for drug screening. [7]

One of the hallmarks of neurodegenerative diseases is the presence of characteristic disease specific protein aggregates. In the case of ALS, these abnormal protein aggregates are mainly composed of phosphorylated and ubiquitinated TDP-43. This imbalance of TDP-43 homeostasis is thought to drive cellular toxicity through the sequestration of the protein, limiting its functionality. Current methods to assess TDP-43 cellular protein homeostasis include Western Blot, immunofluorescence, immunohistochemistry and enzyme-linked immunosorbent assay (ELISA). However, the direct quantification of TDP-43 aggregates and associated proteins that co-aggregate with TDP-43 is not straightforward. Blood derived cells, notably lymphocytes, constitute an easily accessible and unique source for biomarker discovery, and have been previously used to study biological signatures in neurodegenerative diseases such as ALS. [8],[9] In pursuit of a methodology that enables their study and use as a drug screening platform for ALS, Martin-Requero and colleagues implemented a lymphocyte immortalization technique that generates lymphoblasts in culture. [10] Cells recapitulated some aspects of the disease, notably TDP-43 hyperphosphorylation and mislocalization to the cytoplasm. [4]

In 2017, a simple method to measure protein aggregation in different neurodegenerative diseases across cellular models, transgenic animals and human brains, demonstrated that control specimens displayed less protein aggregation than the pathological samples. [11] Here, we use this methodology to measure the propensity for protein aggregation in a bank of lymphoblasts from ALS patients, developing a platform to screen several promising ALS drugs, from protein kinase inhibitors to agents that inhibit protein aggregation. To validate that the effect of drugs on peripheral cells is relevant to ALS, we have measured the molecular aggregation in iPSC-derived motor neurons from ALS patients. Not only is this model a valuable approach to identify whether potential drug candidates can modulate the aggregation observed in ALS patients, but, given the ease with which samples can be acquired in a clinical setting, has the potential to inform drug selection in individual patients.

RESULTS AND DISCUSSION

Immortalized ALS lymphocytes were used to characterize the propensity of proteome aggregation for each of the cell lines. Aggregation was assessed as turbidity measurements, by registering the absorbance of cell extracts diluted in water at a constant protein concentration of 0.75 mg mL^{-1} as reported before. [11] Absorbance measurements were performed at 0, 24, 48 and 72 h. Data were generated for each of the samples and grouped by disease classification averaging the values of all individuals. Figure 1 shows how absorbance measurements increase considerably at 24 h and then either remain stable or show different degrees of incremental values. From the first measurement point at 24 h a clear difference can be observed between control and sporadic ALS patients' immortalized lymphocytes. This difference increases over time reaching statistical significance at 48 and 72 h. The lymphoblasts derived from genetic ALS patients show a more varied molecular aggregation profile. *SOD1* and *TARDBP*

lymphoblasts do not show a difference from controls at 24 h, however they reach a notable difference from controls at 72 h. On the other hand, the samples analyzed for *C9orf72* and *TBK1* patients presented a slight increase over the controls.

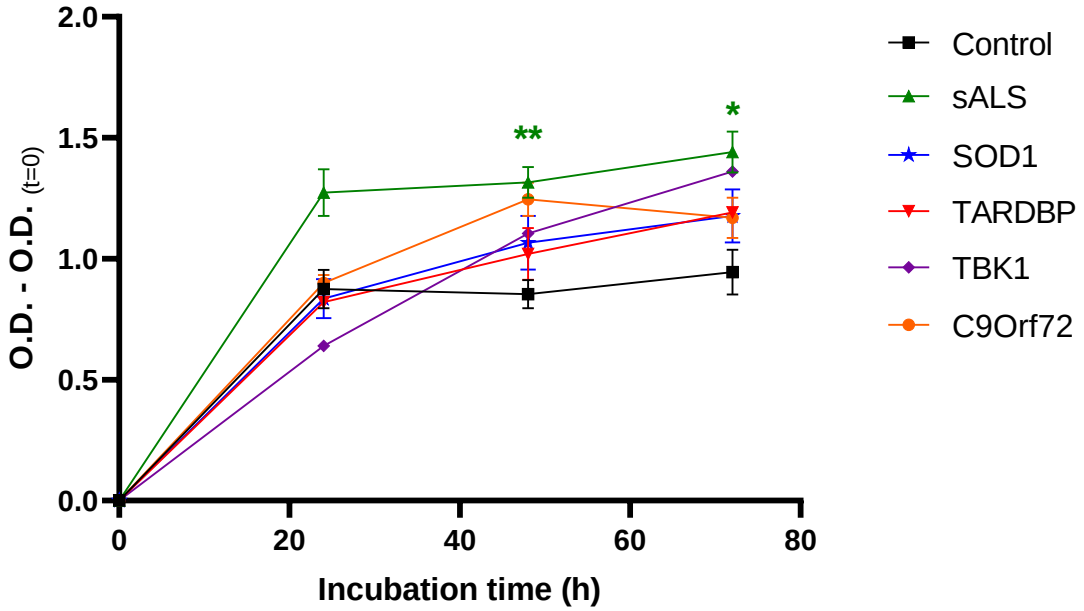

Figure 1. Global proteome turbidity in lymphoblasts from ALS patients. Variation of absorbance at 340 nm with time of the incubated protein extracts obtained from the lymphoblast model of ALS patients and controls. Absorbance was measured at 340 nm for all samples at 0, 24, 48 and 72 h and is here depicted. Points are the mean values +/- SEM. Data were analyzed by one-Way ANOVA with Dunnett comparison test of the different groups of patients with the controls at each time point (*: $p < 0.05$; **: $p < 0.01$).

In order to better illustrate the personalized molecular aggregation profile of all the patients' lymphoblasts included in the study, normalized absorbance measurements at 24 and 72 h are depicted in Figure 2 for all the individual lymphoblastic lines studied.

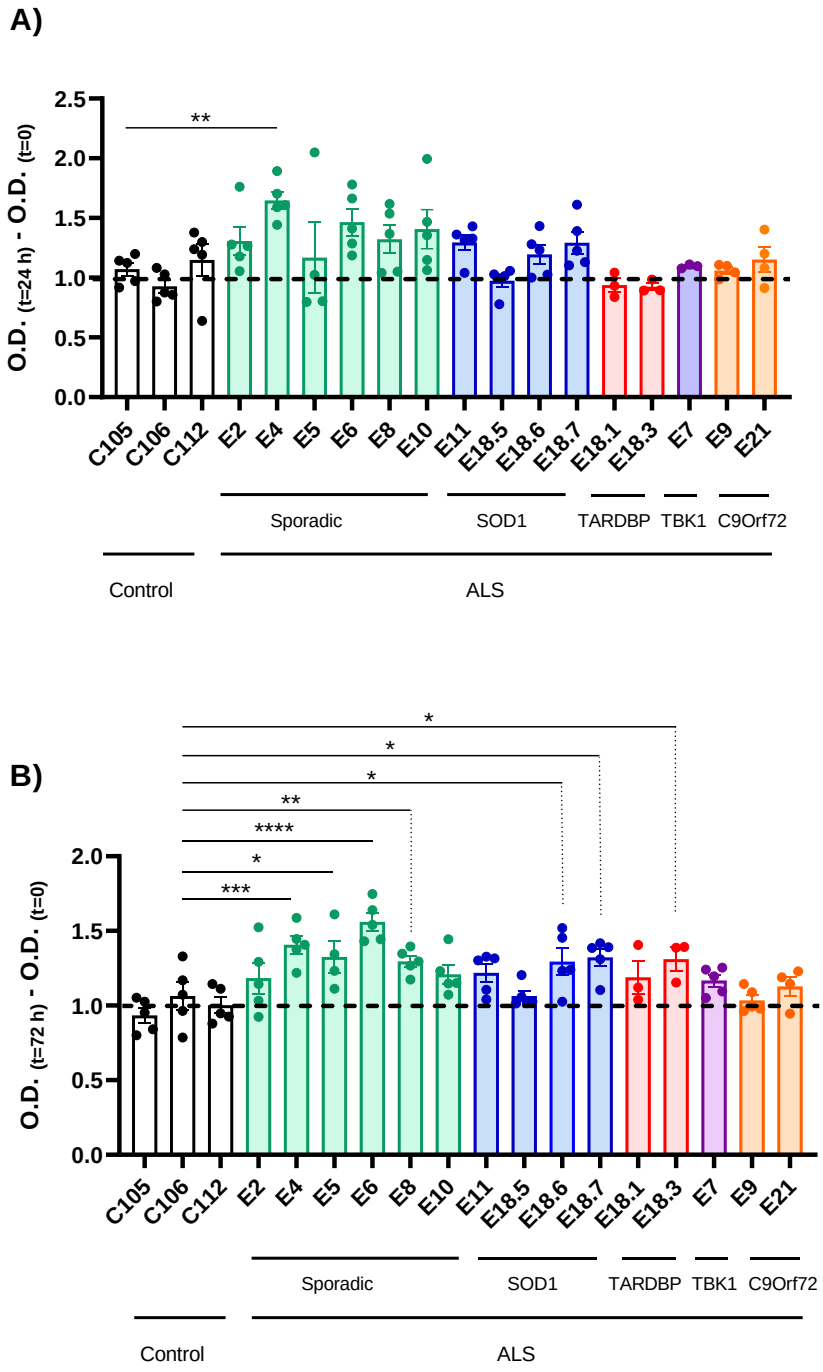

Figure 2. Normalized absorbance measurements of patient lymphoblasts at 24 h (A) and 72 h (B). Bars represent the mean ± SEM. Each of the points depicted in the graphs represents one biological replicate of the experiment. Statistical analysis was performed through One-way ANOVA with Dunnett comparison test, comparing the mean of each column to the mean of C105 (24 h) and C112 (72 h) for being the control individuals closer to the normalization value (*: $p < 0.05$; ** : $p < 0.01$; ***: $p < 0.001$; ****: $p < 0.0001$).

Figure 2 shows the personalized aggregation profile of each of the immortalized lymphocytes derived from the patients included in this study. All sALS samples show a marked tendency towards an increased aggregation profile in comparison to the control samples. At 72 h, four out of the six samples analyzed presented a statistically significant increase. In the case of *SOD1*, three out of four patients show a higher aggregation, with two of them showing statistical significance. Finally, one of the patients with *TARDBP* mutation additionally showed a significant increase in proteome aggregation propensity.

When the samples are grouped by genotype a clear difference in the aggregation pattern against the analyzed control samples can be seen, showing a more homogeneous profile within groups at 72 h (Figure 3 and S2). Statistical differences can be found between the control group and sALS, *SOD1* and *TARDBP* samples at 72 h.

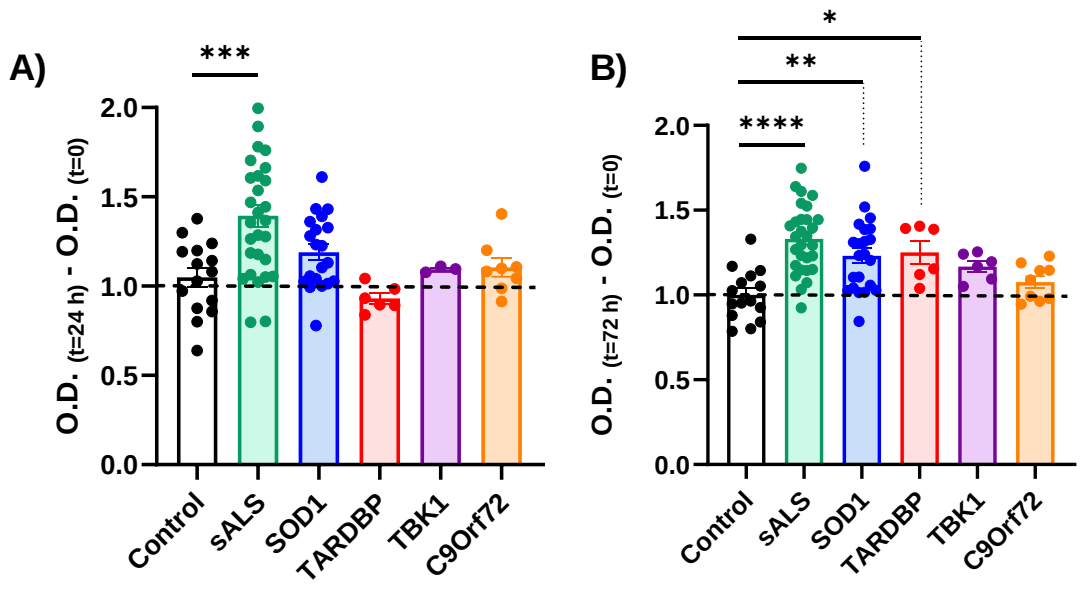

Figure 3. Normalized absorbance measurements of patient lymphoblasts at 24 h (A) and 72 h (B) grouped per disease classification. Bars represent the mean ± SEM. Each of the points depicted in the graphs represents one independent biological experiment of a patient sample. Statistical analysis was performed through One-way ANOVA with

Dunnett comparison test, comparing the mean of each column to the mean of the control group (*: $p < 0.05$; ** : $p < 0.01$; ***: $p < 0.001$; ****: $p < 0.0001$).

With these results at hand, we next explored whether this methodology could serve as a platform for testing drug candidates to study their capacity of modulating aggregate formation. We selected promising therapeutic candidates with different mechanisms of action to test in our model. In particular, we selected four protein kinase inhibitors, 3 aggregation inhibitors of amyloid-prone proteins [15], and tubastatin A (HDAC6 inhibitor) [16] (Figure 4). The protein kinase inhibitors inhibit specific kinases: CK1-δ (IGS2.7), CDC-7 (ERP2.37), TTBK1 (VNG1.47) and GSK-3β (tideglusib), that have been related to the pathological hyperphosphorylation of TDP-43. These drugs had already shown efficacy in several disease models, rescuing ALS phenotypes in cell culture and in animal models [4], [17], [18], [19], [20]. DONE2TCl, HUP7ANTRA, and DP-128 have been shown to inhibit the aggregation of one or several amyloid-prone proteins involved in neurological and non-neurological disorders, including β-amyloid (Aβ42), tau, α-synuclein (α-syn), prion protein (PrP), transthyretin (TTR), and human islet amyloid polypeptide (hIAPP), among others, thereby behaving as amyloid pan-inhibitors. [21], [22] Finally, Ts3ubastatin A, a HDAC6 inhibitor, improved axonal transport in hiPSC derived motor neurons from ALS patients, and also ameliorated the disease in a FUS animal model. [23], [24]

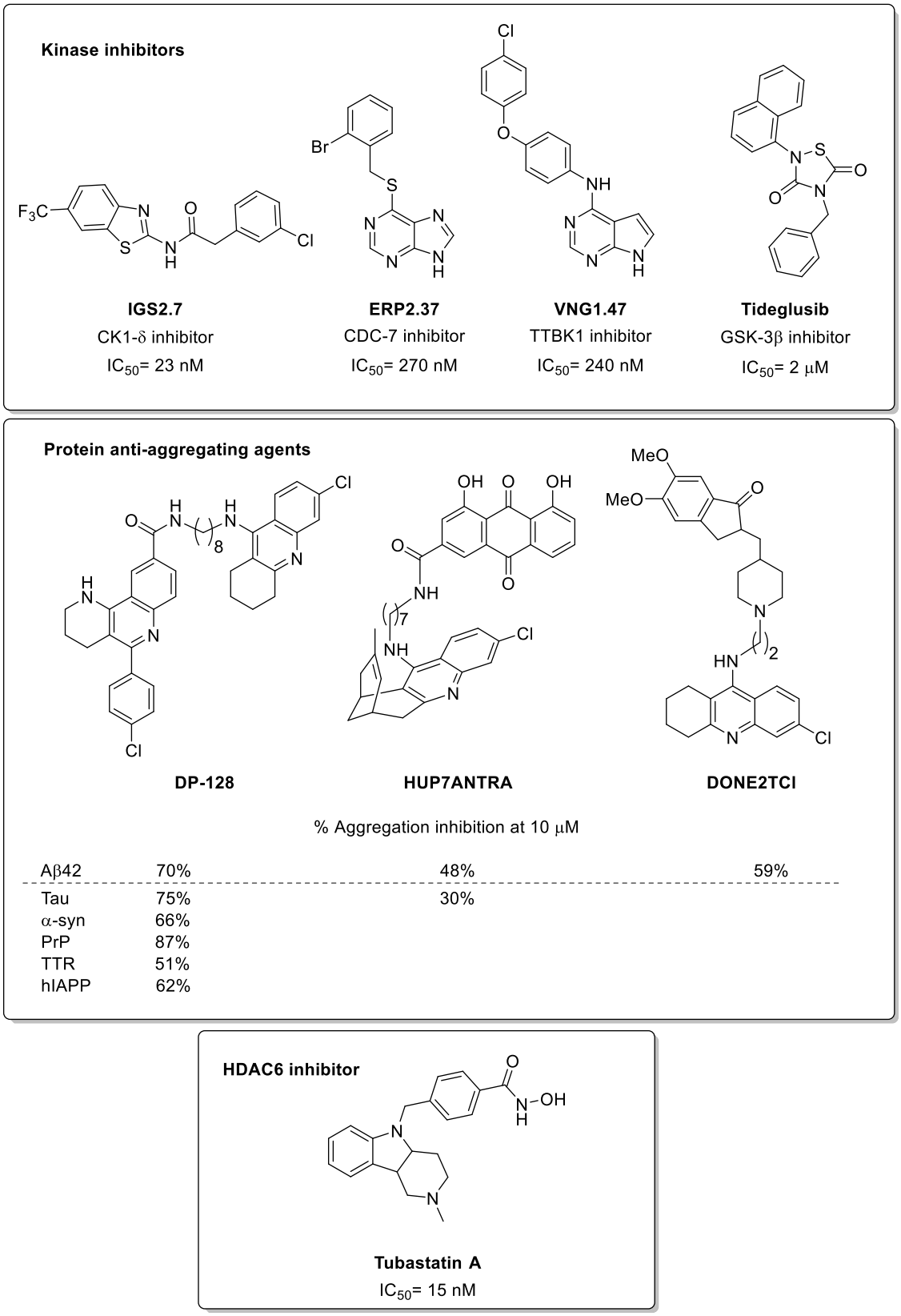

Figure 4. Chemical structure, target and activity data of the drugs evaluated in ALS patient samples.

For the aggregation experiments, cells were treated with the compounds at 5 μM for 24 h, after which, cell lysis and protein quantification were performed. Extracts were diluted and incubated at 37 ºC, measuring absorbance at 340 nm every 24 h. Results are shown in Figure 5, and grouped per disease classification in Figure S3 of the Supporting Information.

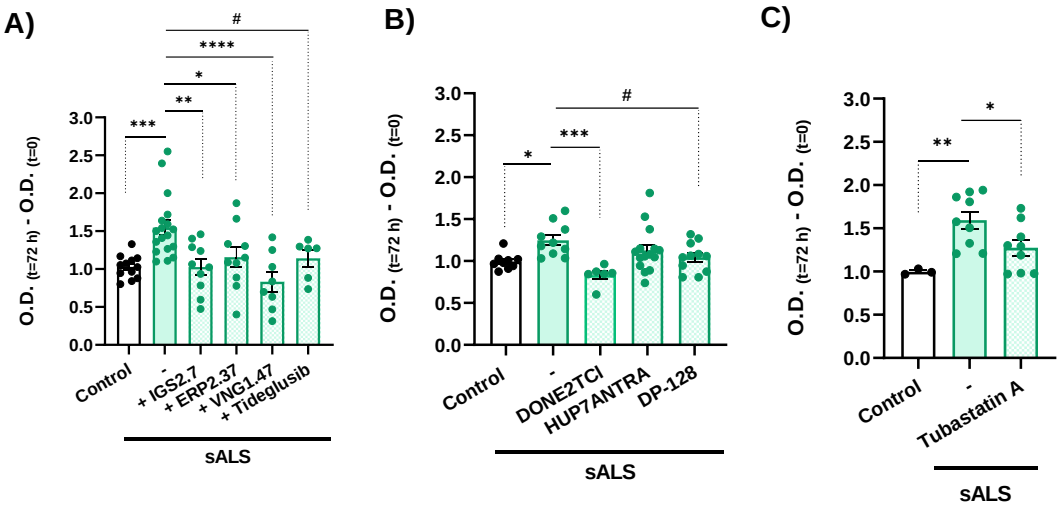

Figure 5. Normalized absorbance measurements of sporadic ALS patient lymphoblasts with or without pharmacological treatment at 72 h A-C. Drug treatments with kinase inhibitors (A), TDP-43 anti-aggregating agents (B), or HDAC-6 inhibitor (C). Bars represent the mean ± SEM. Each of the points depicted in the graphs A-C represents one independent biological experiment of a patient sample. Statistical analysis was performed through One-way ANOVA with Dunnett comparison test, comparing the mean of each column to the mean of sALS (#: $p < 0.1$, *: $p < 0.05$, ** : $p < 0.01$; ***: $p < 0.001$; ****: $p < 0.0001$).

Figure 5 shows how some of the treatments used were efficient in modulating the propensity for molecular aggregation found in the sALS samples. Interestingly, all kinase inhibitors led to a clear reduction of protein aggregation, reaching statistical significance for inhibitors IGS2.7, ERP2.37 and VNG1.47, together with a marked tendency for

tideglusib. These results accord with the known activity of these compounds in inhibition of their respective protein kinases. These enzymes are related to TDP-43 hyperphosphorylation and their inhibition leads to reduced levels of p-TDP-43 in different models. Here it can be observed that inhibition of TDP-43 hyperphosphorylation results in a lower molecular aggregation in ALS patient samples. Inhibitor VNG1.47 achieved the highest reduction in aggregation (49%) while treatment with IGS2.7, ERP2.37 and Tideglusib resulted in a reduction of 32%, 36% and 28% respectively. The compounds that disturb protein aggregation also led to a lower turbidity profile compared to untreated samples, reaching statistical significance for DONE2TCl and a marked tendency for DP-128. DONE2TCl yielded an aggregation reduction of 37% and DP128 of 20%.Finally, the tested HDAC6 inhibitor also showed a significantly reduced number of molecular aggregates of 20%, however it was not efficient enough to reduce the aggregation to the control levels.

Grouped data indicate a significant reduction of pathological aggregates upon treatment, however, when the data are considered at the individual patient level it can be observed that not all of them showed a similar reduction of protein aggregation. In fact, some samples did not seem to benefit from treatment, strikingly those displaying a lower pathological aggregation (see Figure S3 in the Supporting Information). In addition, the effect on molecular aggregation on control samples exerted by the compounds was studied for some of the small molecules (Figure S4), observing no statistical differences.

Next, we decided to investigate the modulation of molecular aggregation in the subset of immortalized lymphocytes from genetic ALS patients, *SOD1*, *TARDBP* and *TBK1*, that presented an increased aggregation in comparison to controls. For these experiments, we selected the most preclinically advanced kinase inhibitors IGS2.7 and ERP2.37, and results are depicted in Figure 6.

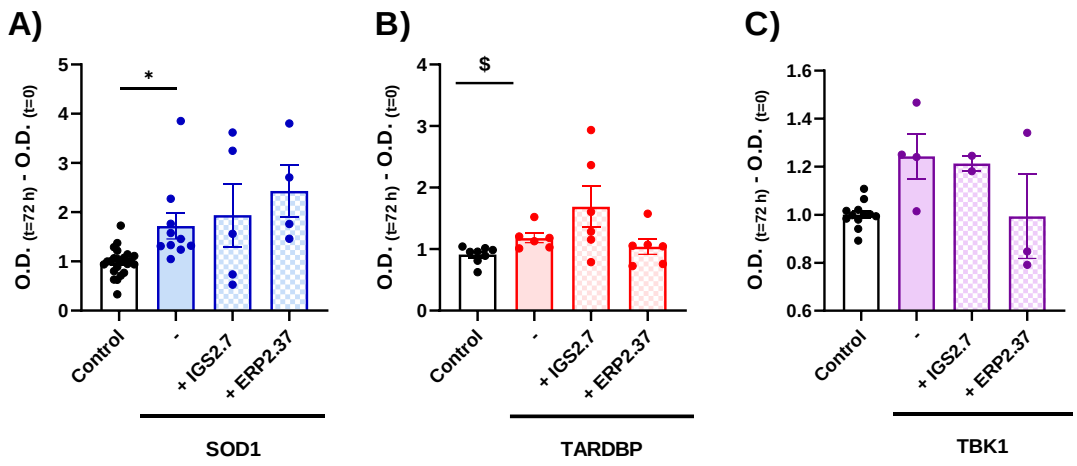

Figure 6. Normalized absorbance measurements of genetic ALS patient lymphoblasts with or without pharmacological treatment at 72 h. *SOD1* patients (A) *TARDBP* patients (B) and *TBK1* patient (C). Bars represent the mean ± SEM. Each of the points depicted in the graphs A-C represents one biological experiment of a patient. Statistical analysis was performed through One-way ANOVA with Tukey comparison test, comparing the mean of each column to the mean of fALS *: $p < 0.05$). In the case of TARDBP $ represents a value of $p < 0.01$ in an umpaired t test comparing patient and control samples.

In the case of these genetic ALS patients we found more heterogeneous results among patients (see Figure S5 of the Supporting Information), and casein kinase inhibitor treatment (IGS2.7) did not decrease protein aggregation in these samples. However, compound ERP2.37 showed a tendency to reduce the aggregation found in the *TBK1* patient. For the *SOD1* and *TARDBP* patients, the inability of kinase inhibitors to reduce aggregates agrees with their mechanism of action, based on TDP43 modulation, a pathological hallmark that is absent in *SOD1* patients. In addition, it illustrates the importance of performing personalized analysis for patient classification and drug administration.

Finally, we decided to assess the propensity towards molecular aggregation in iPSC derived motor neurons (iPSC-MN). iPSC from 2 different ALS patients carrying mutations

on *TARDBP* (I383T and M337V) and from 2 healthy controls were differentiated into motor neurons using a previously published protocol.[13] As described above, aggregation was determined by measuring absorbance at 340 nm of diluted cell extracts at a final concentration of 0.75 mg mL^{-1}.

In this case we did not observe an increase on the absorbance measured at 340 nm, nor even at the final point at 72 h on patients compared to the healthy control (data not shown). However, when analyzing the aggregation rate, we observed that one of the *TARDBP* patients presented a statistically significant increase of molecular aggregation in comparison to the controls (Figure 7). This result is in concordance with the subtle differences observed in this disease model that could represent a prodromal or initial stage of ALS.

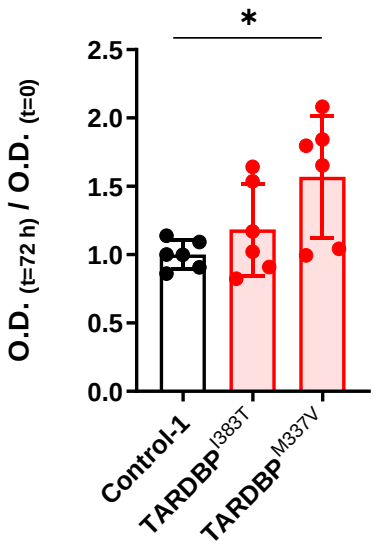

Figure 7. Relative absorbance measurements (Abs_{72h}/Abs_{0h}) for control and disease motoneurons derived from genetic (*TARDBP* I383T and M337V) ALS patients. Bars represent the mean ± SEM. The experiment was performed using three different neuronal differentiations of each sample. Statistical analysis was performed through One-way ANOVA with Dunnett comparison test, comparing the mean of each column to the mean of control-1. (*: $p < 0.05$)

CONCLUSION

Here we have used a simple methodology to measure protein aggregation in several lymphoblastic lines derived from ALS patients and healthy controls. We have observed how turbidity measurements reflect the disease in these patient samples, both in sporadic and genetic forms of the disease. After validation of the model in our samples and given the possibility of having patient's lymphoblasts in culture, we investigated the anti-aggregation profile of several drug candidates that have shown promising pharmacological results *in vitro* and *in vivo*. Results showed how some of these drug candidates were able to decrease molecular aggregation, with this behavior being dependent on the drug and the patient. Interestingly, while protein kinase inhibitors significantly reduced protein aggregation in sALS lymphoblasts, they were not able to produce the same robust effect in genetic ALS patients, which highlights the heterogeneity of the disease and the necessity of tailoring drug treatments to provide improved effects. Finally, we attempted to apply this methodology to measure the proteome homeostasis in motor neurons derived from patients. In this case, while an increase of turbidity was not observed at the final point, a difference was observed at the rate of aggregate formation. With this new methodology we aim to provide a simple and personalized method for disease characterization and biological evaluation in ALS drug discovery.

MATERIALS AND METHODS

Reagents

RPMI 1640 culture media Cat#: L0500 was obtained from Biowest/Labclinics (Barcelona, Spain), Fetal Bovine Serum (FBS) Cat#: F7524 was purchased in Merck (Madrid, Spain), penicillin/streptomycin Cat#: 15140-122 from Gibco/Thermo Fisher (Waltham, MA,

USA). Cell lysis was performed using Nonidet P40 lysis buffer Cat#: J19628 in combination with Pierce Protease and Phosphatase Inhibitor Tablets Cat#: A32959 from Thermo Scientific (Madrid, Spain). Protein quantification was performed with Pierce BCA Protein Assay Kit (Thermo Fisher, Waltham, MA, USA).

Subjects

Peripheral blood samples were obtained after informed consent of the patients or healthy individuals listed in Table 1. All study protocols were approved by the Hospital Doce de Octubre and the Spanish National Research Council Institutional Review Board in accordance with National and European Union Guidelines. A diagnosis of ALS was made in accordance with the revised El Escorial criteria. [12] All iPSC lines were derived from skin biopsy fibroblasts following previously described protocols, [13] and collected under ethical approval granted by the South Wales Research Ethics Committee (WA/12/0186), and reprogrammed in the James Martin Stem Cell Facility, University of Oxford.

Lymphoblastic cell lines

Lymphoblastoid cell lines were established in our laboratory as previously described, by infecting peripheral blood lymphocytes with the Epstein-Barr virus [14], [4] It is important to note that, while several lymphocyte specimens were collected, not all immortalization procedures resulted in stable cell lines. Here we show results of the lymphocytes that underwent a successful immortalization and could be cultured. Lymphoblasts were maintained in culture for a maximum of 12 weeks and were thereafter discarded.

A total of 18 lymphoblastoid lines were included in this study: 3 healthy subjects (C105, C106, C112), 6 sporadic ALS (sALS) patients (E2, E4, E5, E6, E8, E10), and 9 familial ALS (fALS) patients, with mutations in *SOD1* (E11, E18.5, E18.6, E18.7), *TARDBP* (E18.1, E18.3), *C9orf72* (E9 and E21) and *TBK1* (E7). The clinical and demographic details of the patients are presented in Table 1. Lymphoblastoid cell lines from patients

and healthy controls are stored in the biobank of the Center of Biological Research (CIB-CSIC).

Table 1. Clinical and demographic characteristics of the donors. Individuals C105, C106 y C112 have no signs of ALS, individuals E2, E4, E5, E6, E8, E10 have been diagnosed with sALS, and individuals E11, E18.5, E18.6, E18.7, E7, E18.1, E18.3, E9 and E21 are patients with fALS with different mutations. Abbreviations: F, female; M, male; NA, not applicable.

Patient ID	Clinical presentation	Gender	Age at sample obtention	Mutation
C105	NA	F	54	NA
C106	NA	F	57	NA
C112	NA	M	71	NA
E2	Bulbar	F	76	NA
E4	Bulbar	F	54	NA
E5	Spinal	F	54	NA
E6	Bulbar	M	79	NA
E8	Respiratory	M	55	NA
E10	Bulbar	M	68	NA
E11	Spinal	F	64	*SOD1* p.N65S het.
E18.5	Spinal	M	46	*SOD1* p.L117V het.
E18.6	Spinal	M	58	*SOD1* p.N139H het.
E18.7	Spinal	M	59	*SOD1* het p. L117V
E7	Spinal	M	70	*TBK1* p.R573G het.
E18.1	Respiratory	M	59	*TARDBP* p.I383V Het
E18.3	Spinal	M	40	*TARDBP* Hom. p.G295S
E9	Spinal	M	45	*C9orf72* Expansion. Southern *C9orf72* (1894) repeats
E21	Spinal	M	78	*C9orf72* >30 repeats

Cells were grown in suspension using 25 cm^2 flasks vertically oriented, with RPMI-1640 media supplemented with 2 mM L-glutamine, 100 µg mL^{-1} streptomycin/penicillin and

10% (v/v) fetal bovine serum (FBS). Flasks were maintained in an incubator humidified with 5% CO_2 at 37 ºC. Cell media was changed every 3 days by centrifuging cells at 1200 rpm for 5 minutes, removing the medium above the pellet of cells and replacing it with fresh media.

Motor neuron differentiation from human induced pluripotent stem cells

Motor neuron differentiation from iPSC was performed using a previously published protocol, [13] with some modifications. iPSCs were grown on Matrigel (StemCell Technologies) in mTESR™ 1 supplemented with mTESR™ (StemCell Technologies) and antibiotics (Life Technologies). Basal medium during the differentiation process was composed of: DMEM/F12:Neurobasal medium 1:1 (Thermo Fisher Scientific), antibiotic-antimycotic (1X, Thermo Fisher Scientific), N2 supplement (1X, Thermo Fisher Scientific), B27 supplement (1X, Thermo Fisher Scientific), ascorbic acid (0.5 µM, Merck) and β-mercaptoethanol (β-ME, 50 µM, Thermo Fisher Scientific) and then components were changed at different times of the differentiation process (figure 8).

Once iPSCs were 80-90% confluent, induction was started by adding the induction medium containing Chrir99021 (3 µM, R&D Systems) and compound C (1 µM, Merck). After two days in culture, retinoic acid (1 µM, Merck) and smoothened agonist (SAG, 500 nM, R&D Systems) were added to the media. On day 4, Chirr99021 and compound C were removed. On day 9, the neural precursors were split 1:3 using Accutase (Life Technologies) and Rock inhibitor (Y-27632 dihydrochloride, 10 µM, R&D Systems) was added for 24 h. Then, the neural precursors were maintained until day 19, when cells were seeded on 6 well plates coated with Matrigel. Differentiation medium was supplemented with laminin (0.5 µg mL^{-1}, Thermo Fisher Scientific), BDNF (10 ng mL^{-1} Thermo Fisher Scientific), glial cell-derived neurotrophic factor (GDNF, 10 ng mL^{-1} Thermo Fisher Scientific), and DAPT (10 µM, R&D Systems). On day 25, DAPT was removed from the medium. For each patient, two different iPSC-MN lines were analyzed.

Analysis was performed between day 32-37 of the differentiation protocol in all experiments. Full medium changes were then performed every three days.

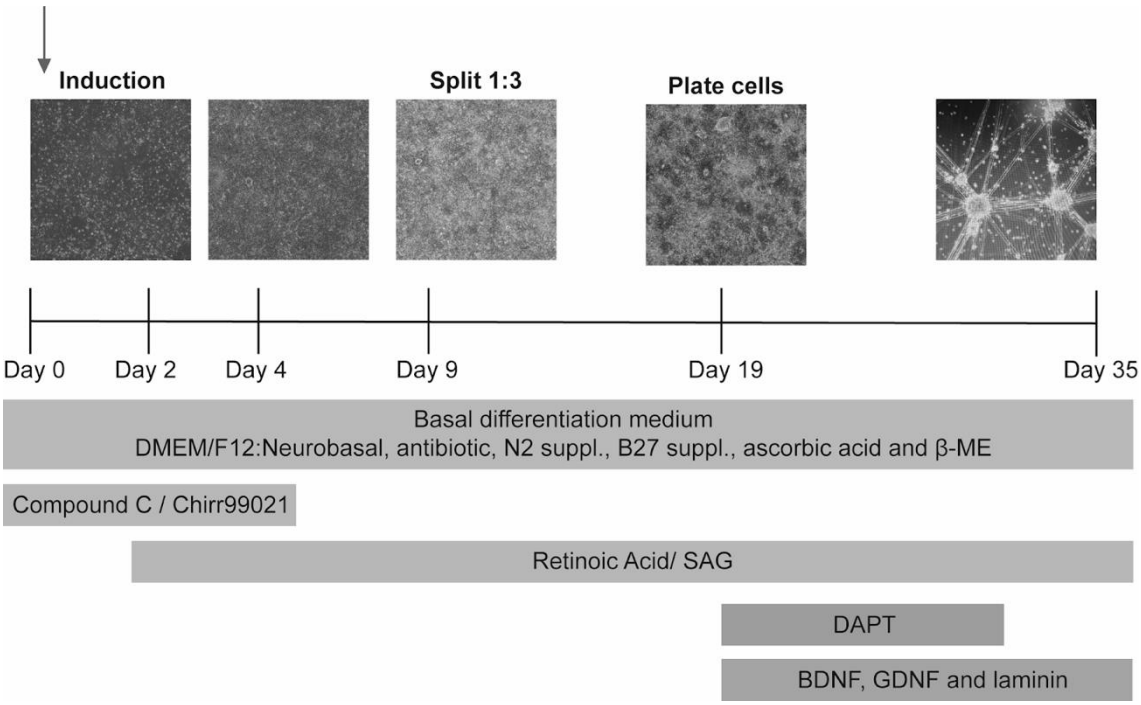

Figure 8. Protocol overview for iPSC-MN differentiation. Exemplary images of the cells at critical time points of the differentiation are shown.

Incubation with drugs and preparation of cellular extracts

Drugs used were: 1) kinase inhibitors IGS2.7, ERP2.37, VNG1.47 and tideglusib, 2) agents that inhibit protein aggregation DP-128, HUP7ANTRA and DONE2TCl; and 3) the HDAC6 inhibitor tubastatin A (Figure 4). Kinase inhibitors were synthesized in the laboratory of Prof. Ana Martinez and protein aggregation modulators in the laboratory of Prof. Diego Muñoz-Torrero. Tubastatin A were obtained from Sigma.

The treatment with the drugs was performed by seeding the cells in a concentration of 1 million cells per mL and incubating with the different drugs at the desired concentration (5 µM) in DMSO for 24 h. DMSO concentration was always maintained below 1% and controls were treated with the same amount of DMSO solution as vehicle. After this time, the media was removed, and cells were washed with cold PBS. The lysis of the cells was

achieved using NP40 lysis buffer in combination with a cocktail of protease and phosphatase inhibitors and performing a centrifugation of 14 000 g at 4 ºC for 15 minutes.

Turbidity assay

The concentration of protein used for the turbidity assay was 0.75 g L^{-1}, which was quantified from cell lysates using the BCA protein quantification assay. Lysates were diluted using milliQ water and were incubated for a total time of 72 h at 37 ºC, measuring turbidity every 24 h. Turbidity of the samples was quantified by absorbance measurements at 340 nm in cuvettes using a Cary 60 UV-Vis Spectrophotometer from Agilent Technologies. Each sample was gently shaken before recording and measured three times.

Data acquisition and statistical analysis

Data was obtained for all absorbance measurements subtracting the value of the blank. Data was normalized to the median average of the controls for every experiment. In a typical assay, controls', patients' and treated patients' lymphoblasts were performed in the same experimental assay. At least three biological replicates (n=3) were performed for all the data points obtained. Statistical analyses were performed with Graph Pad Prism 9. Data sets were tested for normal distribution and passed the Shapiro-Wilk test. All the statistical data are presented as mean ± standard error of the mean (SEM). The statistical test used to assess differences between groups was One-Way ANOVA with the multiple comparisons test indicated in the figure caption of each case. Graph points in grouped representations represent the patients analyzed, each one with a characteristic symbol maintained for the different treatment representation.

AUTHOR CONTRIBUTION

V.P. conceived the research idea, planned the experiments and obtained funding. C.P.L, C.T.B. planned and performed the experiments with support of G.P. D.M.T., and A.M. provided the chemical compounds utilized in the study. R.D and K.T. contributed to the

implementation of the research with motor neurons. C.P.L, C.T.B. and V.P. analyzed and interpreted the data. A.M.R., A.M. D.M.T. and K.T. contributed to the interpretation of the results. V.P. took the lead in writing the manuscript with active support from C.P.L, C.T.B, D.M.T., K.T. and A.M. All authors supervised and contributed to the final version of the manuscript.

FUNDING

This work was partially funded by grant RYC2019-027489-I, Fundación la Caixa ("LCF/ TR/CI19/52460012" "LCF/BQ/PR18/11640007" and "HR21−00931"), grants RYC2019−027489-I, PID2021−128340OA-I00 and PID2020−118127RB-I00, funded by MCIN/AEI/10.13039/501100011033 and by "ESF Investing in your future" (grant RYC2019−027489-I) and "European Union NextGenerationEU/PRTR" (PID2021−128340OA-I00). C.T.B. thanks Ministerio de Educación (FPU18/06310) for the predoctoral fellowship and EMBO Short-Term Fellowship Exchange Program (8856).

NOTES

The authors declare no competing financial interest

SUPPORTING INFORMATION

Supporting information contains the viability measurements of lymphoblastoid cell lines treated with the compounds, the normalized absorbance measurements of patient lymphoblasts grouped by disease classification and after drug treatment in sporadic and genetic patients and aggregation results from treated control lymphoblastoid cell lines.

ACKNOWLEDGEMENTS

We are grateful to the patients, healthy volunteers and clinicians involved in this study for providing samples for research.

REFERENCES

(1) Hardiman, O.; Al-Chalabi, A.; Chio, A.; Corr, E. M.; Logroscino, G.; Robberecht, W.; Shaw, P. J.; Simmons, Z.; van den Berg, L. H. Amyotrophic lateral sclerosis. *Nat Rev Dis Primers* **2017**, *3*, 17071. DOI: 10.1038/nrdp.2017.71.

(2) Kiernan, M. C.; Vucic, S.; Talbot, K.; McDermott, C. J.; Hardiman, O.; Shefner, J. M.; Al-Chalabi, A.; Huynh, W.; Cudkowicz, M.; Talman, P.; et al. Improving clinical trial outcomes in amyotrophic lateral sclerosis. *Nat Rev Neurol* **2021**, *17* (2), 104-118. DOI: 10.1038/s41582-020-00434-z.

(3) Hawrot, J.; Imhof, S.; Wainger, B. J. Modeling cell-autonomous motor neuron phenotypes in ALS using iPSCs. *Neurobiol Dis* **2020**, *134*, 104680. DOI: 10.1016/j.nbd.2019.104680.

(4) Posa, D.; Martinez-Gonzalez, L.; Bartolome, F.; Nagaraj, S.; Porras, G.; Martinez, A.; Martin-Requero, A. Recapitulation of Pathological TDP-43 Features in Immortalized Lymphocytes from Sporadic ALS Patients. *Mol Neurobiol* **2019**, *56* (4), 2424-2432. DOI: 10.1007/s12035-018-1249-8.

(5) Burley, S.; Beccano-Kelly, D. A.; Talbot, K.; Llana, O. C.; Wade-Martins, R. Hyperexcitability in young iPSC-derived C9ORF72 mutant motor neurons is associated with increased intracellular calcium release. *Sci Rep* **2022**, *12* (1), 7378. DOI: 10.1038/s41598-022-09751-3.

(6) Penney, J.; Ralvenius, W. T.; Tsai, L. H. Modeling Alzheimer's disease with iPSC-derived brain cells. *Mol Psychiatry* **2020**, *25* (1), 148-167. DOI: 10.1038/s41380-019-0468-3.

(7) Aversano, S.; Caiazza, C.; Caiazzo, M. Induced pluripotent stem cell-derived and directly reprogrammed neurons to study neurodegenerative diseases: The impact of aging signatures. *Front Aging Neurosci* **2022**, *14*, 1069482. DOI: 10.3389/fnagi.2022.1069482.

(8) Luotti, S.; Pasetto, L.; Porcu, L.; Torri, V.; Elezgarai, S. R.; Pantalone, S.; Filareti, M.; Corbo, M.; Lunetta, C.; Mora, G.; et al. Diagnostic and prognostic values of PBMC proteins in amyotrophic lateral sclerosis. *Neurobiol Dis* **2020**, *139*, 104815. DOI: 10.1016/j.nbd.2020.104815.

(9) Dong, X.; Nao, J.; Shi, J.; Zheng, D. Predictive Value of Routine Peripheral Blood Biomarkers in Alzheimer's Disease. *Front Aging Neurosci* **2019**, *11*, 332. DOI: 10.3389/fnagi.2019.00332.

(10) Alquezar, C.; Salado, I. G.; de la Encarnacion, A.; Perez, D. I.; Moreno, F.; Gil, C.; de Munain, A. L.; Martinez, A.; Martin-Requero, A. Targeting TDP-43 phosphorylation by Casein Kinase-1delta inhibitors: a novel strategy for the treatment of frontotemporal dementia. *Mol Neurodegener* **2016**, *11* (1), 36. DOI: 10.1186/s13024-016-0102-7.

(11) Shmueli, M. D.; Hizkiahou, N.; Peled, S.; Gazit, E.; Segal, D. Total proteome turbidity assay for tracking global protein aggregation in the natural cellular environment. *J Biol Methods* **2017**, *4* (2), e69. DOI: 10.14440/jbm.2017.148.

(12) Brooks, B. R.; Miller, R. G.; Swash, M.; Munsat, T. L.; World Federation of Neurology Research Group on Motor Neuron, D. El Escorial revisited: revised criteria for the diagnosis of amyotrophic lateral sclerosis. *Amyotroph Lateral Scler Other Motor Neuron Disord* **2000**, *1* (5), 293-299. DOI: 10.1080/146608200300079536.

(13) Dafinca, R.; Scaber, J.; Ababneh, N.; Lalic, T.; Weir, G.; Christian, H.; Vowles, J.; Douglas, A. G.; Fletcher-Jones, A.; Browne, C.; et al. C9orf72 Hexanucleotide Expansions Are Associated with Altered Endoplasmic Reticulum Calcium Homeostasis and Stress Granule Formation in Induced Pluripotent Stem Cell-Derived Neurons from

Patients with Amyotrophic Lateral Sclerosis and Frontotemporal Dementia. *Stem Cells* **2016**, *34* (8), 2063-2078. DOI: 10.1002/stem.2388.

(14) Hussain, T.; Mulherkar, R. Lymphoblastoid Cell lines: a Continuous in Vitro Source of Cells to Study Carcinogen Sensitivity and DNA Repair. *Int J Mol Cell Med* **2012**, *1* (2), 75-87.

(15) Espargaro, A.; Pont, C.; Gamez, P.; Munoz-Torrero, D.; Sabate, R. Amyloid Pan-inhibitors: One Family of Compounds To Cope with All Conformational Diseases. *ACS Chem Neurosci* **2019**, *10* (3), 1311-1317. DOI: 10.1021/acschemneuro.8b00398.

(16) Stoklund Dittlau, K.; Krasnow, E. N.; Fumagalli, L.; Vandoorne, T.; Baatsen, P.; Kerstens, A.; Giacomazzi, G.; Pavie, B.; Rossaert, E.; Beckers, J.; et al. Human motor units in microfluidic devices are impaired by FUS mutations and improved by HDAC6 inhibition. *Stem Cell Reports* **2021**, *16* (9), 2213-2227. DOI: 10.1016/j.stemcr.2021.03.029.

(17) Martinez-Gonzalez, L.; Rodriguez-Cueto, C.; Cabezudo, D.; Bartolome, F.; Andres-Benito, P.; Ferrer, I.; Gil, C.; Martin-Requero, A.; Fernandez-Ruiz, J.; Martinez, A.; et al. Motor neuron preservation and decrease of in vivo TDP-43 phosphorylation by protein CK-1delta kinase inhibitor treatment. *Sci Rep* **2020**, *10* (1), 4449. DOI: 10.1038/s41598-020-61265-y.

(18) Nozal, V.; Martinez-Gonzalez, L.; Gomez-Almeria, M.; Gonzalo-Consuegra, C.; Santana, P.; Chaikuad, A.; Perez-Cuevas, E.; Knapp, S.; Lietha, D.; Ramirez, D.; et al. TDP-43 Modulation by Tau-Tubulin Kinase 1 Inhibitors: A New Avenue for Future Amyotrophic Lateral Sclerosis Therapy. *J Med Chem* **2022**, *65* (2), 1585-1607. DOI: 10.1021/acs.jmedchem.1c01942.

(19) Martinez-Gonzalez, L.; Gonzalo-Consuegra, C.; Gomez-Almeria, M.; Porras, G.; de Lago, E.; Martin-Requero, A.; Martinez, A. Tideglusib, a Non-ATP Competitive Inhibitor of GSK-3beta as a Drug Candidate for the Treatment of Amyotrophic Lateral Sclerosis. *Int J Mol Sci* **2021**, *22* (16). DOI: 10.3390/ijms22168975.

(20) Rojas-Prats, E.; Martinez-Gonzalez, L.; Gonzalo-Consuegra, C.; Liachko, N. F.; Perez, C.; Ramirez, D.; Kraemer, B. C.; Martin-Requero, A.; Perez, D. I.; Gil, C.; et al. Targeting nuclear protein TDP-43 by cell division cycle kinase 7 inhibitors: A new therapeutic approach for amyotrophic lateral sclerosis. *Eur J Med Chem* **2021**, *210*, 112968. DOI: 10.1016/j.ejmech.2020.112968.

(21) Camps, P.; Formosa, X.; Galdeano, C.; Gómez, T.; Muñoz-Torrero, D.; Scarpellini, M.; Viayna, E.; Badia, A.; Clos, M. V.; Camins, A.; et al. Novel Donepezil-Based Inhibitors of Acetyl- and Butyrylcholinesterase and Acetylcholinesterase-Induced β-Amyloid Aggregation. *Journal of Medicinal Chemistry* **2008**, *51* (12), 3588-3598. DOI: 10.1021/jm8001313.

(22) Viayna, E.; Sola, I.; Bartolini, M.; De Simone, A.; Tapia-Rojas, C.; Serrano, F. G.; Sabaté, R.; Juárez-Jiménez, J.; Pérez, B.; Luque, F. J.; et al. Synthesis and Multitarget Biological Profiling of a Novel Family of Rhein Derivatives As Disease-Modifying Anti-Alzheimer Agents. *Journal of Medicinal Chemistry* **2014**, *57* (6), 2549-2567. DOI: 10.1021/jm401824w.

(23) Guo, W.; Naujock, M.; Fumagalli, L.; Vandoorne, T.; Baatsen, P.; Boon, R.; Ordovas, L.; Patel, A.; Welters, M.; Vanwelden, T.; et al. HDAC6 inhibition reverses axonal transport defects in motor neurons derived from FUS-ALS patients. *Nat Commun* **2017**, *8* (1), 861. DOI: 10.1038/s41467-017-00911-y.

(24) Rossaert, E.; Pollari, E.; Jaspers, T.; Van Helleputte, L.; Jarpe, M.; Van Damme, P.; De Bock, K.; Moisse, M.; Van Den Bosch, L. Restoration of histone acetylation ameliorates disease and metabolic abnormalities in a FUS mouse model. *Acta Neuropathol Commun* **2019**, *7* (1), 107. DOI: 10.1186/s40478-019-0750-2.